Structure and properties of two glucose-based deep eutectic systems

Fernando Bergua[a], Ignacio Delso[b], José Muñoz-Embid[a], Carlos Lafuente[a], Manuela Artal[a,*]

[a]Departamento de Química Física, Instituto Agroalimentario de Aragón-IA2 (Universidad de Zaragoza-CITA), Zaragoza, Spain

[b]Departamento de Síntesis y Estructura de Biomoléculas, Instituto de Síntesis Química y Catálisis Homogénea (ISQCH), Universidad de Zaragoza-CSIC, Spain

*Corresponding author. Tel: +34876553765. e-mail: martal@unizar.es

Abstract

Continued industrialization and increasing environmental problems have highlighted the need to research new eco-friendly solvents, also known as deep eutectic solvents (DESs). To implement these solvents in industrial processes, the knowledge of their molecular organization and thermophysical properties must be enhanced. In this work, two DESs have been characterized: d-glucose:choline chloride:water (GCH) and d-glucose:citric acid:water (GCiH). NMR techniques were used to analyse both the supramolecular structure and the role of water and to calculate the diffusion coefficients. Moreover, seven thermophysical properties at several temperatures were evaluated. As a second aim, the solubility of quercetin was determined. NMR studies showed a stronger supramolecular structure of GCH and a high ratio of β-glucose in both DESs. Based on the thermophysical results, the solvent with choline chloride had the most compact fluid structure. Finally, the solubility of quercetin in the DESs was higher than in water, especially for GCH.

Keywords: Choline chloride; Glucose; Citric acid; Quercetin; Thermophysical properties; Solubility

1. Introduction

A significant number of traditionally used solvents present technical (volatility, reactivity, solubility in phases, etc.) and environmental problems. Initially, ionic liquids were proposed as an alternative, but their high cost and toxicity have prevented their implementation. Since 2003 (Abbott, Capper, Davies, Rasheed &Tambyrajah, 2003), deep eutectic solvents (DESs) have been studied as new eco-sustainable solutions, especially those classified as Type III. They are formed by an organic salt, typically an ammonium halide, and organic acids, or sugars, among others compounds. These DESs exhibit characteristics that are consistent with several of the requirements of green chemistry: a negligible vapor pressure, a high solvent capacity, biodegradability, tuneability, and cheap and efficient preparation (Clarke, Tu, Levers, Bröhl & Hallett, 2018; Paiva, Matias & Duarte, 2018). As more essential information regarding these mixtures becomes known, the number of industrial processes that incorporate these eco-friendly solvents will increase considerably in the near future.

A correct pharmaceutical formulation requires the optimization of the final product including the active principle (APIs), the drug vehicle, and excipients. This statement can also be extended to the dietary supplement (nutraceutical) industry. To achieve this goal, it is essential to study the interactions between the components of the final product and the measure of its physicochemical properties. In the future, all of these aspects could follow an efficient design of tailor-made formulations. The bioavailability of the APIs and poorly water-soluble nutraceutical compounds is one of the challenges faced by the pharmaceutical industry (Hauss, 2007; Kalepu & Nekkanti, 2015; Singh, Worku, & Van den Mooter, 2011). Almost half of the commercially approved APIs and most of those in development have solubility problems in aqueous media (Kalepu & Nekkanti, 2015). In this way, the possibilities of oral liquid formulations, which are preferred for patients with swallowing difficulties, are limited. In contrast, it may also be suitable to increase the hydrophobic character of APIs that are extremely soluble in water, such as the vitamin B12, to establish an adequate lipid balance. Different strategies with the aim of improving the pharmacokinetic properties

of drugs have been developed: the use of saline-derived APIs is preferred to the use of acid-derived as well as amorphous forms instead of crystalline, the addition of co-solvents, encapsulation in micelles, the formation of inclusion complexes that are usually based on cyclodextrins, nanoparticle technologies, self-emulsifying drug delivery systems (SEDDS), and ordered mesoporous silica (OMS) (Singh et al., 2011). In 1998, Stott et al. (Stott, Williams, & Barry, 1998) studied eutectic mixtures of ibuprofen with terpenes obtaining an increase of the permeability of the drug. More recently, deep eutectic solvents (DESs) containing different APIs have been studied to obtain liquid forms of high concentration. The utility of both hydrophilic and hydrophobic DESs as a new pathway that improves the bioavailability of active principles has been proved (Duarte et al., 2017; Formula et al., 2018; Morrison, Sun & Neervannan, 2009; Shekaari, Zafarani-Moattar, Shayanfar, & Mokhtarpour, 2018; Silva, Reis, Paiva, & Duarte, 2018). Quercetin (Q) is the most abundant flavonoid in nature and possesses, among others, antioxidant, anti-viral, anti-obesity, and anti-carcinogenic activities (Wang et al., 2016). However, both its low solubility in aqueous media and poorly stability are two substantial handicaps confronting the use of quercetin as a drug or diet supplement (Abraham & Acree, 2014). To increase the Q bioavailability, several methods have been proposed. Wang et al. (Wang et al., 2016) published an interesting review regarding the activity, stability, and delivery methods of quercetin. We propose that the use of deep eutectic solvents as solubility enhancers can be added to the methods indicated in that article (Dai, van Spronsen, Witkamp, Verpoorte, & Choi, 2013; López, Delso, Matute, Lafuente, & Artal, 2019).

Here, two glucose-based DESs are studied: glucose:choline chloride:water (1:3:3, mole ratio) (GCH) and glucose:citric acid:water (1:1:6.5, mole ratio) (GCiH). These aqueous solvents have shown high efficacy in the food and biotechnology industry (Benvenutti, Zielinski & Ferreira, 2019; Dai et al., 2013; Mišan et al., 2019; Tang, Zhong, & Yan, 2016; Zainal-Abidin, Hayyan, Hayyan, & Jayakumar, 2017), extraction of bioactive products (flavonoids, terpenes, and isoflavones, among others), solubility of poorly water soluble compounds, removal of metals from food, and phase

change materials (PCMs) for energy storage (especially for food storage). The sugar:choline chloride DESs have shown a high biodegradability and biocompatibility so they are considered to be benign solvents, whereas those based on an organic acid have exhibited antimicrobial activity but lower toxicity than the conventional solvents (Zhao et al., 2015). No toxicological studies have been found concerning glucose:citric acid mixtures. Pisano et al. (Pisano, Espino, Fernández, Silva, & Olivieri, 2018) have studied the structure of GCiH and some papers have reported physicochemical data for both systems (Aroso, Paiva, Reis, & Duarte, 2017; Dai et al., 2013; Dai, Witkamp, Verpoorte, & Choi, 2015; Florindo, Oliveira, Branco, & Marrucho, 2017; Hayyan et al., 2013; Moghimi & Roosta, 2019; Silva, Fernandez, & Coutinho, 2018; Tang et al., 2016). However, their compositions do not match with those proposed here. The GCH concentration was chosen to quantify the effect of increasing the choline chloride ratio. Silva et al. (Silva et al., 2018) characterized the glucose:choline chloride (1:1, mole ratio) system. Herein, we have increased the choline chloride ratio while maintaining a similar water content (8% wt). The composition of the GCiH solvent is similar to that previously studied by our team (López et al., 2019), except with choline chloride instead of glucose. Thus, we can evaluate the effect of the replacement between both components. The purpose of this paper is to analyse two aqueous eutectic solvents with glucose and either choline chloride or citric acid. First, we use NMR spectroscopy to characterize the H-bonding network, define the role of water in both liquids, and determine the diffusion coefficients. Second, we measure and calculate several thermophysical properties. Finally, we evaluate the solubility of quercetin in both DESs to confirm the solvent capability of these mixtures.

2. Experimental

2.1. Materials

The chemicals were acquired from Sigma-Aldrich and used as supplied, with the exception of choline chloride. Because of its highly hygroscope nature, the choline chloride was dried under

vacuum before utilization. The water content of the choline chloride, as measured by the Karl-Fischer method, was 1250 ppm, which was taken account when calculating its composition. The resistivity of the added Milli-Q water was less than 18.2 μS·cm^{-1}. The mixtures were prepared by weighing (BP210S Sartorius balance, $u(m)$=0.1 mg) and subsequent heating with magnetic stirring. The studied compositions were: glucose:choline chloride:water (1:3:3) and glucose:citric acid:water (1:1:6.5). The acronyms used throughout this paper to identify these solvent mixtures are GCH and GCiH, respectively.

Table S1 (Supplementary material) provides information regarding the pure compounds, and Table S2 lists the characteristics of the studied DESs: the acronyms used in this work, the compositions, the water content (W), and the molar mass (M).

2.2. Apparatus and procedure

2.2.1. NMR Experiments

A Bruker AVANCE spectrometer operating at 400 MHz was used to perform NMR experiments at 298 K; the chemical shifts were referenced to tetramethylsilane. Eight scans were recorded with a standard one-pulse sequence (Bruker pulse program zg) for each ^{1}H-NMR spectrum, and 256 scans were collected with an APT sequence (Bruker pulse program *jmod*) for each ^{13}C-NMR. Signal assignment was performed with a routine gradient of selected DQF-COSY, ^{1}H-^{13}C HSQC, and ^{1}H-^{13}C HMBC signals. The characterization was completed with Nuclear Overhauser Effect SpectroscopY (NOESY) and Diffusion-Ordered SpectroscopY (DOSY) experiments. More details are reported in the Supplementary Data. Using the DOSY technique, the self-diffusion coefficients (D) were calculated from:

$$I(g) = I_0 \exp[-D\gamma_H^2 g^2 \delta^2 (\Delta - \delta/3)] \quad (1)$$

where $I(g)$ and I_0 are the resonance intensity measured for a given gradient strength, g, and in its absence; γ_H is the gyromagnetic ratio of the hydrogen nucleus; δ is the duration of the bipolar gradient pulse; and Δ is the observation time.

2.2.2. Thermophysical Properties

An Anton Paar DSA 5000 (3 MHz) apparatus was used to measure both the densities (ρ) and speed of sound (u) of the mixtures. Apparatus calibration was performed with dry air and ultrapure water (SH Calibration Service GmbH). An Abbemat-HP refractometer, calibrated with Milli-Q water, was used to determine the refractive indices at the sodium D wavelength (n_D). The isobaric molar heat capacities ($C_{p,m}$) were obtained with a DSC Q2000 (TA Instruments) calorimeter using the zero-heat flow procedure and a synthetic sapphire sample as the reference system. The surface tensions (γ) were measured with a drop volume tensiometer (Lauda TVT-2). The measurements were performed in a closed container to limit water adsorption. A Schoot-Geräte AVS-440 automatic measuring unit along with several Ubbelohde capillary viscometers (of varying inner diameter) were used to determine kinematic viscosities (ν), and from ρ and ν data, the dynamic viscosity, $\eta = \rho \cdot \nu$, was calculated. Finally, a CRISON conductimeter (model GLP31), calibrated with KCl aqueous solutions supplied by CRISON, was utilized to measure the electrical conductivities (σ). All apparatuses were thermostatted and the standard uncertainties are: $u(T)$=0.005 K for the Anton Paar device and 0.01 K for the remaining. In the measured properties, the combined expanded uncertainties (0.95 level of confidence, k=2) are: $U_c(\rho)$=0.05 kg·m^{-3}; $U_c(u)$=0.5 m·s^{-1}; $U_c(n_D)$=2·10^{-5}; $U_c(C_{p,m})$=1%; $U_c(\gamma)$=1%; $U_c(\eta)$=1%; $U_c(\sigma)$=1%.

At least two sets of measurements with different batches of mixture were performed for each technique of characterization. The values reported in this work are the average data.

2.2.3. Solubility Measurements

The quercetin solubility was determined by using the shake-flask method with thermostatted double-walled flasks protected from light degradation with foil. The solute was added to each flask until the point of super saturation, and then, the flask was stirred for 24 h at 298.15 K. After sedimentation, three aliquots of each flask were separately centrifuged and filtered (PES syringe filter, 0.22 μm). Each result is the average value of six analyses. The Q concentration was determined using UV-VIS spectroscopy (double-beam spectrum VWR 6300 PC, $u(\lambda)$=±0.2 nm) by diluting the mixture in ethanol. The quercetin solubility expressed as a mass fraction (W_{Q}) was calculated with the following calibration curve obtained (López et al., 2019) at λ=372-374 nm, and the peak of maximum absorption: $A = 52556.9 \cdot W_{\mathrm{Q}}$.

3. Results and Discussion

3.1. NMR study

A structural study of GCH and GCiH using several NMR techniques is presented below. Spectra for diluted mixtures with deuterated water (D_2O) are also included. Both the nuclei and the interactions between components are identified. In aqueous DESs, to evaluate the role of water, the relevant question is: Do these mixtures have a supramolecular structure involving hydrogen bond donor (HBD), an acceptor (HBA), and water molecules or, in contrast, are they aqueous solutions? Different authors (Delso, Lafuente, Muñoz-Embid, & Artal, 2019; Hammond, Bowron, & Edler, 2017) have shown that water, in a moderate amount, contributes to establishing the H-bond network. An increase of the water content weakens the structure until the point of collapse into an aqueous solution. We use several abbreviations in this text: aliphatic hydrogens of glucose (G), hydroxyl hydrogens of glucose ($\mathrm{OH-G}$), aliphatic hydrogens of choline ($\mathrm{Ch^+}$), hydroxyl hydrogen of choline ($\mathrm{OH-Ch^+}$), aliphatic hydrogens of citric acid (Ci), hydroxyl hydrogens of citric acid ($\mathrm{OH-Ci}$), and hydrogens of water (W).

3.1.1. GCH

The presence of two anomeric forms of glucose, α-glucose and β-glucose, complicates the explanation of hydrogen and carbon spectra. In the ^{1}H-NMR spectrum (Fig. 1a), the signals of G (e, g, i, k, m, n), $OH-G$ (f, h, j, l, o), Ch^{+} (b, c, d), $OH-Ch^{+}$(a), and W (p) are separated, which indicates that hydrogens are not involved in fast exchange processes, possibly because they are fixed within a H-bond network. In addition, the $OH-G$ peaks corresponding to the α and β anomers are differentiated. In the ^{13}C spectrum (Fig. 1b), the aliphatic carbons of both anomers can also be identified. Diluting GCH (10% DES + 90% D_2O), the resolution of the ^{1}H spectrum is enhanced and all mobile hydrogens coalesce into the signal for hydrogen-deuterium oxide (Fig. S1a). The fast exchange of hydrogens indicates that the H-bond network has been dissolved. From ^{13}C (Fig. S1b), the change of the chemical shifts in the dilution process is: $\Delta\delta$ [(δ-^{13}C GCH) – (δ-^{13}C diluted GCH)]: +0 C_b, +0.1 C_c, +0 C_d, +0.1 $C_{e\alpha}$, +0.4 $C_{g\alpha}$, +0.2 $C_{i\alpha}$, +0.3 $C_{k\alpha}$, +0.5 $C_{m\alpha}$, +0.2 $C_{n\alpha}$, +0.4 $C_{e\beta}$, +0.7 $C_{g\beta}$, +0.5 $C_{i\beta}$, +0.4 $C_{k\beta}$, +0.6 $C_{m\beta}$, +0.4 $C_{n\beta}$. It can be seen that the β-glucose chemical environment was more affected by dilution. Furthermore, in the GCH solvent, the calculated ratio of β/α is 61.5/38.5, while in the diluted mixture, this ratio increases to 63.3/36.7. As it is well known, the β anomer is the more stable form in water, with similar observations having also been reported in other choline chloride-based eutectics (Wu et al., 2018). However, the inclusion of glucose as a main component of the DES seems to either enhance the stability of the α anomer or reduce that of the β.

NOESY experiments were performed to evaluate the interactions among the components of the GCH. This technique displays the hydrogens coupling through space. In this experiment, molecular tumbling determines both the intensity and sign of the crosspeaks, such that fast tumbling molecules give positive signals whereas slow ones (large particle size or high viscosity) show stronger and negative NOEs. The corresponding spectra for GCH at the mixing times (t_{mix}) of 50 and 800 ms are shown in Fig. 1c and 1d, respectively, in which all observed signals are negative. The Ch^{+} interacts with both the glucose and water, with the strongest interaction being with $OH-G$, and the result being slightly higher for β-glucose (comparing the ^{1}H and NOESY peaks integrals).

According to these experimental results, it can be proposed that in this highly polar medium, the α-glucose is stabilized, possibly by enhancing the anomeric effect. In contrast, due to its more symmetric conformation, β-glucose seems to fit better in the supramolecular DES network. However, these proposals should be investigated thoroughly and are beyond the scope of this work. The mobility of the different species can be quantified by DOSY spectroscopy, as described in section 2.2.1. In this DES, all species have similar diffusion coefficients (D) indicating a grouped displacement (Table 1 and Fig. 1e). Logically, water has the highest D although it is much lower than in pure water: D_{H_2O}(T=298.15 K)=230·10^{-11} m^2·s^{-1} (Andanson, Traïkia, & Husson, 2014). Therefore, it can be concluded that choline chloride, glucose, and water establish a supramolecular structure in which the β anomer, likely for steric reasons, seems to fit better and may interact strongly. Following Hammond et al. (Hammond et al., 2017), the GCH is a "water-in-DES" system.

3.1.2. GCiH

In this DES, in contrast to GCH, all mobile hydrogens appear in a single signal, that of water (Fig. 2a). Citric acid catalyses the exchange of OH – G (g, I, k, m p, q), OH – Ci (d, e), and W (q), so it is impossible to obtain independent signals. The chemical shifts for the ^{13}C-NMR are shown in Fig. 2b.

By adding 90% D_2O, the spectra become sharper (Fig. S2). However, Δδ could not be calculated, since the presence of the acid reduces the information obtained. Again, the β anomer is also favoured; the β/α ratio is 54.2/43.8 in neat DES and 61.3/38.7 in the diluted solvent. The evaluation of the possible supramolecular structure was performed with NOESY and DOSY experiments. Fig. 2c shows the 2D-NOESY spectrum with a short mixing time, in which several negative nOes appear, with the most intense crosspeaks being among the mobile hydrogens and the aliphatic hydrogens from the citric acid and glucose. Signal enhancement and the arising of new crosspeaks are observed to increase with the mixing time (Fig. 2d). The DOSY spectrum (Fig. 2e) shows that glucose and citric acid move together, indicating the presence of a supramolecular

structure. However, the larger differences between the diffusion coefficients for the several species (especially water) suggest that the structure is weaker than that of GCH (Table 1).

3.2. Thermophysical study

Tables S3 and S4 report the experimental values of several thermophysical properties determined as functions of temperature, at p = 0.1 MPa, in the present study. The properties are the density (ρ), speed of sound (u), refractive index (n_D), isobaric molar capacity ($C_{p,m}$), surface tension (γ), kinematic and dynamic viscosities (ν, η), and electric conductivity (σ). The operating temperature range varied according to the solid transition of each DES: for GCH (T_{tr} ≈295 K, visual appreciation), T=298.15 – 338.15 K, and for GCiH, T=288.15 – 338.15 K. Furthermore, Table S5 lists, at each temperature, the values of the following calculated properties: isobaric expansion coefficient (α_p), isentropic compressibility (κ_s), intermolecular free length (L_f), molar refractivity (R_m), and free volume (f_m). To facilitate the reading of the paper, we have collected the values of the experimental and calculated properties at T=298.15 K in Table 2.

In this section, we compare the results with those for the citric acid:choline chloride:water 1:1:6 molar ratio (CiCH), previously published by our team (López et al., 2019). Thus, the effect on the thermophysical properties of the replacement of choline chloride by glucose in the mixture with citric acid can be evaluated.

3.2.1. Thermodynamic properties

Density, speed of sound, and refractive index all provide information about the structure of a liquid. The liquid's ρ is inversely proportional to the size occupied by one mole of compound. Moreover, u and n_D indicate the molecular packing because emptiness hinders the transmission of sound and facilitates light propagation; thus, the less compact the fluid is, the lower the values of u

and n_D. The increase of the molecular motion due to the temperature increase in the system induces a decrease in the value of these properties (Fig. 3 (a)-(c)). They can be correlated by a linear equation:

$$Y = A_Y + B_Y T \quad (2)$$

where Y is the property, and T is the temperature in Kelvin. The A_Y and B_Y coefficients are the fit parameters, the values of which are listed in Table S6. The measured ρ values indicated that the solvent containing citric acid was approximately 15% denser than that with choline chloride. The influence of the temperature on the density (Fig. 3a) was quantified with the isobaric expansion coefficient, α_p:

$$\alpha_p = -\frac{1}{\rho}\left(\frac{\partial \rho}{\partial T}\right)_p \quad (3)$$

where ρ is the density, and T is the temperature in Kelvin. The obtained values ranged from 0.42 to 0.52 (±0.04) kK^{-1} and were higher for the GCiH solvent. The temperature influence on α_p was negligible. Silva et al. (Silva et al., 2018), Florindo et al. (Florindo et al., 2017), and Tang et al. (Tang et al., 2016) have published the densities of mixtures containing glucose and choline chloride (1:1), with 8, 10, and 38.24 wt% water, respectively. Comparing the two first papers, it can be seen that the density slightly decreases, MRD=0.25%, increasing the water content by 2%. In comparison with our data, the density decreased by increasing the HBA/HBD ratio. Our mixture, which had a molar ratio of 1:3 (W=8%), was approximately 5% lighter than that of Silva et al. (Silva et al., 2018). Dai et al. (Dai et al., 2013) and Zhao et al. (Zhao et al., 2015) studied mixtures with compositions close to that of this paper (1:2.5, molar ratio), and the published values were in agreement with ours. A graphical comparison with citations is shown in Fig. S3a. For the DES with citric acid, the density also decreased with an increase of the water content (Fig. S4a). Finally, the replacement of choline chloride by glucose in the mixture containing citric acid increased the density by more than 10%. The values of the speed of sound were very high, especially for GCH (Fig. 3b). The fluid compressibility under adiabatic conditions (the isentropic compressibility, κ_s) can be calculated from

ρ and u values and allows us to evaluate the available free space into the liquid. In addition, the intermolecular free length (L_f) can be calculated from:

$$L_f = K\sqrt{\kappa_s} = K\sqrt{1/\rho u^2} \quad (4)$$

where K=(91.368+0.3565T)10^{-8} is the Jacobson's constant, a temperature-dependent variable. The calculated values of κ_s and, consequently, L_f were lower for GCH, indicating a more compact structure. For both eutectic mixtures, the compression capacity was highly influenced by T. For GCiH, u data were similar to those measured for CiCH. However, the intermolecular free length was lower due to the effect of the density; at 298.15 K, L_f(CiCH)=0.297 Å.

The above result is in accordance with the determined refractive index values, because a higher degree of compaction in the fluid implies a greater hindrance of light transmission. Fig. 3c shows the n_D linear decrease with temperature increase. From ρ and n_D, the molar refraction (R_m) can be calculated by using the Lorentz-Lorentz relation:

$$R_m = \left(\frac{n_D^2 - 1}{n_D^2 + 2}\right)\frac{M}{\rho} \quad (5)$$

Molar refraction is related to the hard core volume of a mole of molecules. Thus, the free volume (f_m) can be evaluated by the difference between the molar volume (V_m) and the molar refraction. Both the calculated values of the molar refractive and the free volume for the DES with choline chloride were twice those for the other mixture. However, taking into account the corresponding molar volumes, the percentage of unoccupied space was lower: 70.6% for GCH and 72.2% for GCiH. This result in consistent with earlier results: the solvent containing choline chloride exhibited better packaging. Furthermore, the unoccupied volume for GCiH was slightly lower than for the CiCH mixture.

The isobaric molar capacity is also in agreement with the fact that the H-bond network was more important for GCH. Note the very high $C_{p,m}$ values for this DES, which were found to be more than twice those for GCiH and other similar mixtures (Lapeña, Lomba, Artal, Lafuente, & Giner, 2019a,

2019b; López et al., 2019). Eutectic mixtures composed by sugars are studied as alternatives to traditional materials for thermal energy storage at low temperature (Shao et al., 2018). In this field, a high isobaric capacity is a positive datum. The behaviour with the change in temperature was as expected: $C_{p,m}$ increased with increasing T (Fig. 3d), according to the eq. (2).

Surface tension is related to the balance between the cohesion and adhesion forces at the air-liquid interface. The values for GCH were higher than for GCiH. In addition, the γ dependence with T (Fig. 3e) was more pronounced for the first mixture. Table 2 also includes the calculated data of two thermodynamic functions of surface, the entropy and the enthalpy of the surface per unit surface area, ΔS_S and ΔH_S:

$$\Delta S_S = -(\partial\gamma/\partial T)_p \quad (6)$$

$$\Delta H_S = \gamma - T(\partial\gamma/\partial T)_p \quad (7)$$

These properties suggest, respectively, the change in the order of the molecules and the energy to form the interface. As a result, the more structured liquids have greater ΔS_S and ΔH_S values. The values for the DESs studied herein were very high, especially for GCH. In comparison with CiCH, exchanging the choline chloride by glucose contributed to the changes in the liquid's structure.

The critical temperature of a system, T_c, is an important property for carrying out theoretical studies and correlations. However, the experimental measure of T_c in this type of system is very difficult due to the thermal decomposition of the organic compounds. However, an estimated value can be obtained from γ data with the Guggenheim equation and from ρ and γ data using the Eötvos relation:

$$\gamma = \gamma_0 \left(1 - \frac{T}{T_c}\right)^{11/9} \quad (8)$$

$$\gamma \left(\frac{M}{\rho}\right)^{2/3} = K(T_c - T) \quad (9)$$

where γ (mN·m^{-1}) and ρ (kg·m^{-3}) are the experimental data at the temperature T (K); M (kg·mol^{-1}) is the molar mass; and T_c (K) is the critical temperature. γ_0 (mN·m^{-1}), K (J·K^{-1}·mol$^{-2/3}$), and T_c (K) are

the fit parameters listed in Table S7. These equations have already been used to estimate the critical temperatures of some phosphonium-based DESs (Ghaedi, Ayoub, Sufian, Lal, & Shariff, 2017). Rai and Maggin (Rai & Maginn, 2011) showed that despite the simplicity of both equations, the critical temperatures calculated with them, and those obtained from molecular simulation, were in agreement for several ionic liquids. The T_c calculated for GCiH was higher than that for GCH, which could be due to the higher water content of the latter. To evaluate the consistency of the estimated T_c, we have calculated the densities with the modified Rackett equation:

$$\rho = A\, B^{-(1-T/T_c)^{\frac{2}{7}}} \tag{10}$$

where A and B are two fit parameters (Table S7) related to the critical density and compressibility factor, respectively. The high regression values and small mean relative deviations (Table S7) showed that the calculate T_c data can be reliable.

3.2.2. Transport properties

The fluidity of a system is a direct consequence of the size and shape of the molecules composing the system, as well as the presence of interactions within it. The higher viscosity the slower movement of the species; thus, dynamic viscosity (η) and electric conductivity (σ) are two interrelated properties. It can be seen that our mixtures are quite viscous despite their water contents. An increase of the temperature favours mobility, especially at lower T. Thus, the variation of the transport properties with temperature is exponential; in this work, we have used the VFT equation:

$$\eta = A_\eta \exp\left(\frac{B_\eta}{T - C_\eta}\right) \tag{11}$$

$$\sigma = A_\sigma \exp\left(-\frac{B_\sigma}{T - C_\sigma}\right) \tag{12}$$

where T (K) is the temperature, and A_Y, B_Y, and C_Y are the fit parameters (Table S6). A_Y is the contribution to the transport property Y due to molecule size and shape (negligible interactions),

whereas B_Y and C_Y allow for the calculation of the energetic barrier that must be overcome for the transport process, $E_{a,Y}$ (Table 2):

$$E_{a,Y} = R\frac{\partial(lnY)}{\partial\left(\frac{1}{T}\right)} = R\left(\frac{B_Y}{\left(\frac{C_Y^2}{T^2} - \frac{2C_Y}{T} + 1\right)}\right) \quad (13)$$

where R (J·mol^{-1}·K^{-1}) is the universal gas constant. Comparing with our previous paper, the A_η values of GCH and CiCH were similar, such that the steric hindrance in both mixtures was parallel. Furthermore, the $E_{a,\eta}$ of GCiH was slightly higher than that for GCH but was almost double that of CiCH. Therefore, we can say that the lowest viscosity, recorded for GCiH, is mainly due to its lower water content and the fact that the glucose - citric acid interactions were stronger than the choline chloride - citric acid interactions. Figs. S3b, S3c, and S4b show a good agreement between the η and σ literature data and our results for the similar mixtures. The fractional Walden rule allows us to relate the viscosity and the ionic conductivity of a fluid at each p and T:

$$\Lambda_m \cdot \eta^\alpha = C \quad (14)$$

where Λ_m is the molar conductivity ($\Lambda_m = \sigma\, M/\rho$), C is the Walden product, and α is the fractional factor. The two coefficients have been calculated from the linear fitting of the logarithmic expression, as reported in Table S7. Many papers have proposed an interpretation of the ionicity of such solutions using the deviation from the ideal KCl line where the α parameter is unity. However, Schreiner et al. (Schreiner, Zugmann, Hartl, & Gores, 2010) argued that this value was not correct. From the literature data for infinitely dilute aqueous KCl solutions at several T, they found a value of α=0.87. We obtained a similar value for GCH but a very lower ionicity for GCiH. Moreover, the viscosity can also be related to the surface tension with the Pelofsky and Murkerjee equations:

$$\gamma = A_1 \exp\left(\frac{B_1}{\eta}\right) \quad (15)$$

$$\gamma = A_2\, \eta^{\frac{B_2}{3}} \quad (16)$$

where γ (mN·m^{-1}) and η (mPa·s) are the experimental data, and A_i and B_i are empirical coefficients, listed in Table S7. From the regression coefficients, we can say that the Murkerjee equation is the best correlation for our data.

3.3. Quercetin solubility

Flavonoids are a type of compound that are of special interest both in the pharmaceutical and the nutritional industries. However, flavonoids have a poor bioavailability because their solubility in water is very low; for quercetin, Q, the value (in mass fraction) is: $W_Q(\mathrm{H_2O})$=4.3·10^{-7} (López et al., 2019). Conversely, Q is soluble in inadequate solvents as drug vehicles such as methanol, ether, or acetone. Thus, increasing the solubility of quercetin in aqueous solutions is an attractive goal, and several papers have shown that DESs can be a viable alternative (Dai et al., 2013; López et al., 2019). In this work, we have measured the solubility of quercetin at 298.15 K in both studied DESs. The obtained data were: $W_Q(\mathrm{GCH})$=1.78·10^{-2} and $W_Q(\mathrm{GCiH})$=1.05·10^{-4}. These results and those corresponding to other eutectic mixtures are shown in Fig. 4. In all cases, the solubility of quercetin increased considerably in comparison with its solubility in water, with the most suitable solvent being the mixtures with lower water contents. By comparison, we have only found the solubility of quercetin in GCH at 313 K (Dai et al., 2013). Logically, this datum ($W_Q(\mathrm{GCH})$=0.342) is higher than our value due to the effect of temperature.

4. Conclusions

In this paper, we characterized two aqueous deep eutectic solvents, GCH and GCiH, whose compositions were d-glucose:choline chloride:water (1:3:3, molar ratio) and d-glucose:citric acid:water (1:1:6.5, molar ratio), respectively. Several NMR techniques at 298 K were used to prove the existence of a supramolecular structure in these mixtures. Their internal interactions were studied with Nuclear Overhauser Effect Spectroscopy (NOESY), and the movement of the species was quantified by Diffusion-Ordered Spectroscopy (DOSY) experiments. Furthermore, thermodynamic

and transport properties (density, speed of sound, refractive index, isobaric molar capacity, surface tension, kinematic viscosity, and electric conductivity) from 298.15 or 288.15 to 338.15 K and at p = 0.1 MPa were measured and discussed. As a final goal, the capability of both DESs to dissolve quercetin was determined.

From the NMR study, we concluded that the components of each mixture form a supramolecular structure, which was stronger for GCH. In both DESs, the β anomer of glucose was favoured. The thermophysical properties brought the same conclusion: the solvent with choline chloride (GCH) was the most structurally compact fluid. Finally, the solubility of quercetin in the studied mixtures was higher than in water, especially for GCH ($\times 4.1 \cdot 10^4$). This result is related to its high electronic polarizability, which favours the solubility of highly polarizable solutes.

Supplementary data

Supplementary data to this article can be found in the online version.

Acknowledgements

The authors are thankful for the financial support received from Gobierno de Aragón and Fondo Social Europeo (E-54) "Construyendo Europa desde Aragón".

References

Abbott, A. P., Capper, G., Davies, D. L., Rasheed, R. K., & Tambyrajah, V. (2003). Novel solvent properties of choline chloride/urea mixtures. *Chemical Communications*, *9*(1), 70–71. https://doi.org/10.1039/b210714g

Abraham, M. H., & Acree, W. E. (2014). On the solubility of quercetin. *Journal of Molecular Liquids*, *197*, 157–159. https://doi.org/10.1016/j.molliq.2014.05.006

Andanson, J., Traïkia, M., & Husson, P. (2014). Ionic association and interactions in aqueous methylsulfate alkyl-imidazolium-based ionic liquids. *The Journal of Chemical Thermodynamics*, *77*, 214–221. https://doi.org/10.1016/j.jct.2014.01.031

Aroso, I. M., Paiva, A., Reis, R. L., & Duarte, A. R. C. (2017). Natural deep eutectic solvents from choline chloride and betaine – Physicochemical properties. *Journal of Molecular Liquids*, *241*, 654–661. https://doi.org/10.1016/j.molliq.2017.06.051

Benvenutti, L., Zielinski, A. A. F., & Ferreira, S. R. S. (2019). Which is the best food emerging solvent: IL, DES or NADES? *Trends in Food Science and Technology*, *90*(January), 133–146. https://doi.org/10.1016/j.tifs.2019.06.003

Clarke, C. J., Tu, W. C., Levers, O., Bröhl, A., & Hallett, J. P. (2018). Green and Sustainable

Solvents in Chemical Processes. *Chemical Reviews*, *118*(2), 747–800. https://doi.org/10.1021/acs.chemrev.7b00571

Dai, Y., van Spronsen, J., Witkamp, G. J., Verpoorte, R., & Choi, Y. H. (2013). Natural deep eutectic solvents as new potential media for green technology. *Analytica Chimica Acta*, *766*, 61–68. https://doi.org/10.1016/j.aca.2012.12.019

Dai, Y., Witkamp, G. J., Verpoorte, R., & Choi, Y. H. (2015). Tailoring properties of natural deep eutectic solvents with water to facilitate their applications. *Food Chemistry*, *187*, 14–19. https://doi.org/10.1016/j.foodchem.2015.03.123

Delso, I., Lafuente, C., Muñoz-Embid, J., & Artal, M. (2019). NMR study of choline chloride-based deep eutectic solvents. *Journal of Molecular Liquids*, *290*, 111236. https://doi.org/10.1016/j.molliq.2019.111236

Duarte, A. R. C., Ferreira, A. S. D., Barreiros, S., Cabrita, E., Reis, R. L., & Paiva, A. (2017). A comparison between pure active pharmaceutical ingredients and therapeutic deep eutectic solvents: Solubility and permeability studies. *European Journal of Pharmaceutics and Biopharmaceutics*, *114*, 296–304. https://doi.org/10.1016/j.ejpb.2017.02.003

Florindo, C., Oliveira, M. M., Branco, L. C., & Marrucho, I. M. (2017). Carbohydrates-based deep eutectic solvents: Thermophysical properties and rice straw dissolution. *Journal of Molecular Liquids*, *247*, 441–447. https://doi.org/10.1016/j.molliq.2017.09.026

Formula, C., Weight, M., Gutiérrez, A., Atilhan, M., Aparicio, S., Balawejder, M., Mossety-Leszczak, B., Poplewska, I., Lorenz, H., Seidel-Morgenstern, A., Piatkowski, W., Antos, D., Babaei, F., Mirzababaei, M., Nassiri-Asl, M., Li, Z., & Lee, P. I. (2018). Investigation on drug solubility enhancement using deep eutectic solvents and their derivatives. *International Journal of Pharmaceutics*, *346*(9), 8–19. https://doi.org/10.1039/c8cp05641b

Ghaedi, H., Ayoub, M., Sufian, S., Lal, B., & Shariff, A. M. (2017). Measurement and correlation of physicochemical properties of phosphonium-based deep eutectic solvents at several temperatures (293.15 K–343.15 K) for CO2capture. *Journal of Chemical Thermodynamics*, *113*, 41–51. https://doi.org/10.1016/j.jct.2017.05.020

Hammond, O. S., Bowron, D. T., & Edler, K. J. (2017). The Effect of Water upon Deep Eutectic Solvent Nanostructure: An Unusual Transition from Ionic Mixture to Aqueous Solution. *Angewandte Chemie - International Edition*, *56*(33), 9782–9785. https://doi.org/10.1002/anie.201702486

Hauss, D. J. (2007). Oral lipid-based formulations. *Advanced Drug Delivery Reviews*, *59*(7), 667–676. https://doi.org/10.1016/j.addr.2007.05.006

Hayyan, A., Mjalli, F. S., AlNashef, I. M., Al-Wahaibi, Y. M., Al-Wahaibi, T., & Hashim, M. A. (2013). Glucose-based deep eutectic solvents: Physical properties. *Journal of Molecular Liquids*, *178*, 137–141. https://doi.org/10.1016/j.molliq.2012.11.025

Kalepu, S., & Nekkanti, V. (2015). Insoluble drug delivery strategies: Review of recent advances and business prospects. *Acta Pharmaceutica Sinica B*, *5*(5), 442–453. https://doi.org/10.1016/j.apsb.2015.07.003

Lapeña, D., Lomba, L., Artal, M., Lafuente, C., & Giner, B. (2019a). The NADES glyceline as a potential Green Solvent: A comprehensive study of its thermophysical properties and effect of water inclusion. *The Journal of Chemical Thermodynamics*, *128*, 164–172. https://doi.org/10.1016/j.jct.2018.07.031

Lapeña, D., Lomba, L., Artal, M., Lafuente, C., & Giner, B. (2019b). Thermophysical characterization of the deep eutectic solvent choline chloride:ethylene glycol and one of its mixtures with water. *Fluid Phase Equilibria*, *492*, 1–9. https://doi.org/10.1016/j.fluid.2019.03.018

López, N., Delso, I., Matute, D., Lafuente, C., & Artal, M. (2019). Characterization of xylitol or citric acid:choline chloride:water mixtures: Structure, thermophysical properties, and quercetin solubility. *Food Chemistry*, 125610. https://doi.org/10.1016/j.foodchem.2019.125610

Mišan, A., Nađpal, J., Stupar, A., Pojić, M., Mandić, A., Verpoorte, R., & Choi, Y. H. (2019). The perspectives of natural deep eutectic solvents in agri-food sector. *Critical Reviews in Food Science and Nutrition*, 1–29. https://doi.org/10.1080/10408398.2019.1650717

Moghimi, M., & Roosta, A. (2019). Physical properties of aqueous mixtures of (choline chloride + glucose) deep eutectic solvents. *Journal of Chemical Thermodynamics*, *129*, 159–165. https://doi.org/10.1016/j.jct.2018.09.029

Morrison, H. G., Sun, C. C., & Neervannan, S. (2009). Characterization of thermal behavior of deep eutectic solvents and their potential as drug solubilization vehicles. *International Journal of Pharmaceutics*, *378*(1–2), 136–139. https://doi.org/10.1016/j.ijpharm.2009.05.039

Paiva, A., Matias, A. A., & Duarte, A. R. C. (2018). How do we drive deep eutectic systems towards an industrial reality? *Current Opinion in Green and Sustainable Chemistry*, *11*, 81–85. https://doi.org/10.1016/j.cogsc.2018.05.010

Pisano, P. L., Espino, M., Fernández, M. de los Á., Silva, M. F., & Olivieri, A. C. (2018). Structural analysis of natural deep eutectic solvents. Theoretical and experimental study. *Microchemical Journal*, *143*(August), 252–258. https://doi.org/10.1016/j.microc.2018.08.016

Rai, N., & Maginn, E. J. (2011). *Vapor–liquid coexistence and critical behavior of ionic liquids via*. 1439–1443.

Schreiner, C., Zugmann, S., Hartl, R., & Gores, H. J. (2010). Fractional walden rule for ionic liquids: Examples from recent measurements and a critique of the so-called ideal KCl line for the walden plot. *Journal of Chemical and Engineering Data*, *55*(5), 1784–1788. https://doi.org/10.1021/je900878j

Shao, X. F., Wang, C., Yang, Y. J., Feng, B., Zhu, Z. Q., Wang, W. J., Zeng, Y., & Fan, L. W. (2018). Screening of sugar alcohols and their binary eutectic mixtures as phase change materials for low-to-medium temperature latent heat storage. (I): Non-isothermal melting and crystallization behaviors. *Energy*, *160*, 1078–1090. https://doi.org/10.1016/j.energy.2018.07.081

Shekaari, H., Zafarani-Moattar, M. T., Shayanfar, A., & Mokhtarpour, M. (2018). Effect of choline chloride/ethylene glycol or glycerol as deep eutectic solvents on the solubility and thermodynamic properties of acetaminophen. *Journal of Molecular Liquids*, *249*, 1222–1235. https://doi.org/10.1016/j.molliq.2017.11.057

Silva, J. M., Reis, R. L., Paiva, A., & Duarte, A. R. C. (2018). Design of Functional Therapeutic Deep Eutectic Solvents Based on Choline Chloride and Ascorbic Acid [Research-article]. *ACS Sustainable Chemistry and Engineering*, *6*(8), 10355–10363. https://doi.org/10.1021/acssuschemeng.8b01687

Silva, L. P., Fernandez, L., & Coutinho, A. P. (2018). *Design and Characterization of Sugar-Based Deep Eutectic Solvents Using Conductor-like Screening Model for Real Solvents*. https://doi.org/10.1021/acssuschemeng.8b02042

Singh, A., Worku, Z. A., & Van den Mooter, G. (2011). Oral formulation strategies to improve solubility of poorly water-soluble drugs. *Expert Opinion on Drug Delivery*, *8*(10), 1361–1378. https://doi.org/10.1517/17425247.2011.606808

Stott, P. W., Williams, A. C., & Barry, B. W. (1998). Transdermal delivery from eutectic systems: Enhanced permeation of a model drug, ibuprofen. *Journal of Controlled Release*, *50*(1–3), 297–308. https://doi.org/10.1016/S0168-3659(97)00153-3

Tang, N., Zhong, J., & Yan, W. (2016). Solubilities of three flavonoids in different natural deep eutectic solvents at T = (288.15 to 328.15) K. *Journal of Chemical and Engineering Data*, *61*(12), 4203–4208. https://doi.org/10.1021/acs.jced.6b00552

Wang, W., Sun, C., Mao, L., Ma, P., Liu, F., Yang, J., & Gao, Y. (2016). The biological activities, chemical stability, metabolism and delivery systems of quercetin: A review. *Trends in Food Science and Technology*, *56*, 21–38. https://doi.org/10.1016/j.tifs.2016.07.004

Wu, M., Zhou, W., Pedersen, C. M., Ma, H., Qiao, Y., Guo, X., Hou, X., & Wang, Y. (2018).

Isomeric distribution of monosaccharides in deep eutectic solvents: NMR study. *Journal of Molecular Liquids*, *255*, 244–249. https://doi.org/10.1016/j.molliq.2018.01.166

Zainal-Abidin, M. H., Hayyan, M., Hayyan, A., & Jayakumar, N. S. (2017). New horizons in the extraction of bioactive compounds using deep eutectic solvents: A review. *Analytica Chimica Acta*, *979*, 1–23. https://doi.org/10.1016/j.aca.2017.05.012

Zhao, B., Xu, P., Yang, F., Wu, H., Zong, M., & Lou, W. (2015). *Biocompatible Deep Eutectic Solvents Based on Choline Chloride: Characterization and Application to the Extraction of Rutin from Sophora japonica*. https://doi.org/10.1021/acssuschemeng.5b00619.

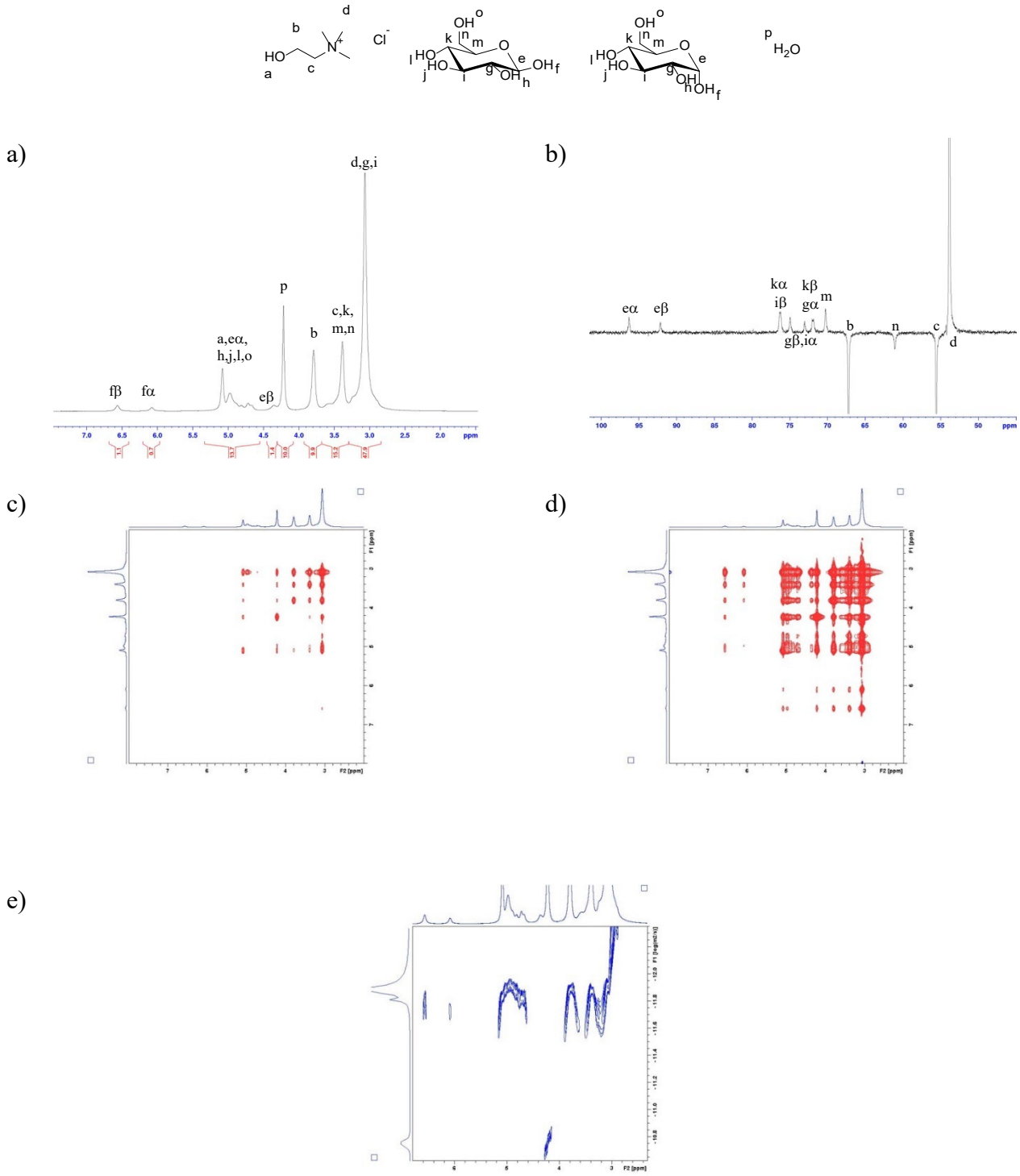

Fig. 1 Spectra recorded at 298.15 K for GCH. a) ^{1}H-NMR: 2.84-3.30 (m, 47.9 H, H_d, H_g, H_i), 3.30-3.68 (m, 15.2 H, H_c, H_k, H_m, H_n), 3.79 (s, 10 H, H_b), 4.21 (s, 10 H, H_p), 4.35 (s, 1.4 H, $H_{e\beta}$), 4.61-5.21 (m, 13.7 H, H_a, $H_{e\alpha}$, H_h, H_j, H_l, H_o), 6.08 (s, 0.7 H, $H_{f\alpha}$), 6.57 (s, 1.1 H, $H_{f\beta}$); b) ^{13}C-NMR: 53.8 (C_d), 55.6 (C_c), 61.1 (C_n), 67.2 (C_b), 70.3 (C_m), 72.0 ($C_{g\alpha}$), 72.0 ($C_{k\beta}$), 73.0 ($C_{i\alpha}$), 75.0 ($C_{g\beta}$), 76.4 ($C_{i\beta}$), 76.4 ($C_{k\alpha}$), 92.1 ($C_{e\beta}$), 96.3 ($C_{e\alpha}$); c) NOESY at t_{mix}=50 ms; d) NOESY at t_{mix}=800 ms; e) DOSY spectrum.

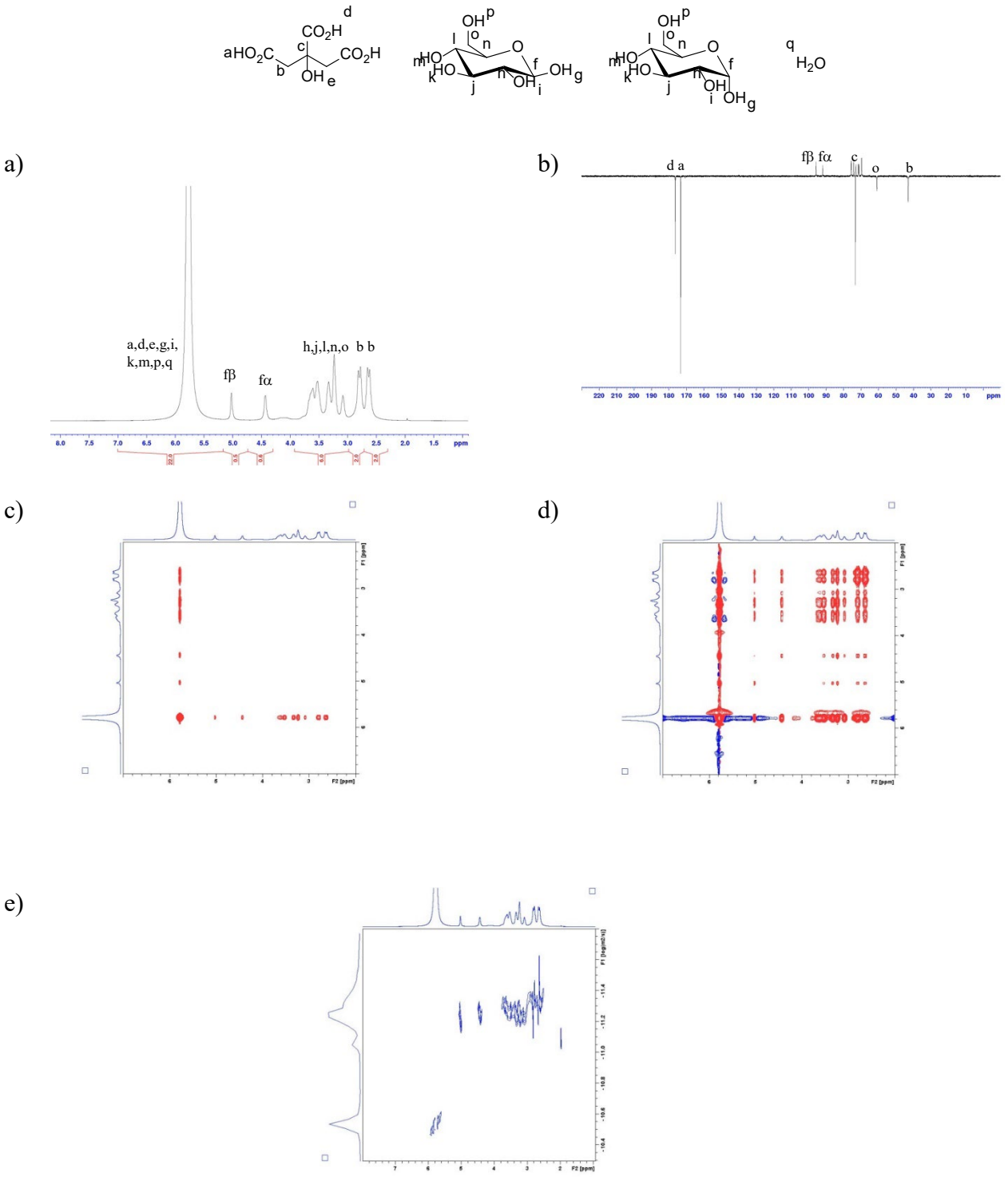

Fig. 2 Spectra recorded at 298.15 K for GCiH. a) ^{1}H-NMR: δ 2.64 (d, J = 14.0 Hz, 2H, H_b), 2.80 (d, J = 14.0 Hz, 2 H, H_b), 3.00-3.85 (m, 6 H, H_h, H_j, H_l, H_n, H_o), 4.43 (s, 0.5 H, $H_{fβ}$), 5.02 (s, 0.5 H, $H_{fα}$), 5.75 (s, 22 H, H_a, H_d, H_e, H_g, H_i, H_k, H_m, H_p, H_q); b) ^{13}C-NMR: 43.0 (C_b), 60.9 (C_o), 69.6, 71.1, 71.4, 72.9, 73.4 (C_c), 74.1, 75.4, 75.6, 91.9 ($C_{fα}$), 95.8 ($C_{fβ}$), 173.2 (C_a), 176.4 (C_d); c) NOESY at t_{mix}=50 ms; d) NOESY at t_{mix}=800 ms; e) DOSY spectrum.

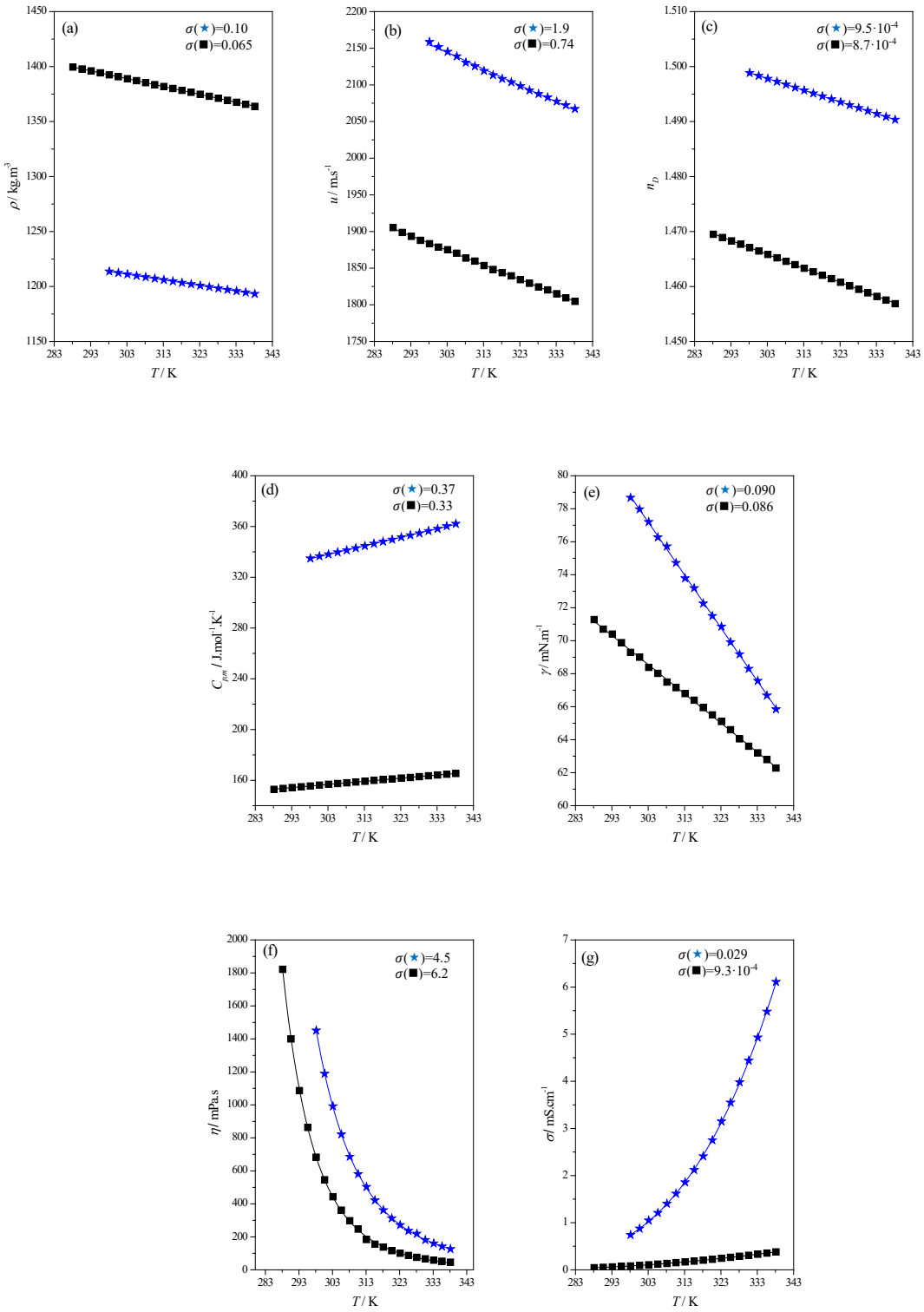

Fig. 3. Thermophysical properties of the studied DESs: (★), GCH; and (■), GCiH. (a) Density; (b) speed of sound; (c) refractive index; (d) isobaric molar heat capacity; (e) surface tension; (f) dynamic viscosity; and (g) electric conductivity. The standard deviation, σ, is included. Points represent experimental values and lines represent correlated data (eqs. 2, 11, and 12).

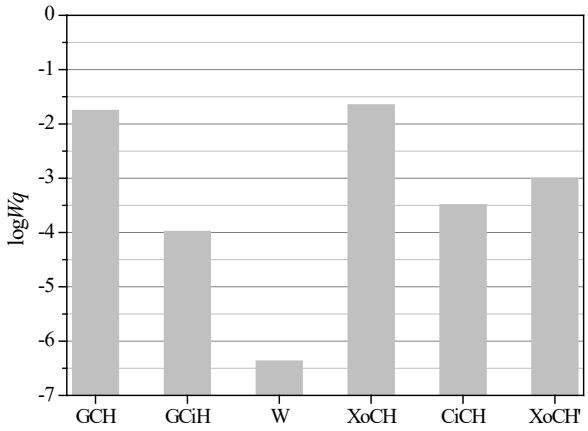

Fig. 4 Solubility (in mass fraction) of quercetin in several deep eutectic solvents at T=298.15 K. GCH, glucose:choline chloride:water (1:3:3) and GCiH, glucose:citric acid:water (1:1:6.5), from this work. W, water; XoCH, xylitol:choline chloride:water (1:2:3); CiCH, citric acid:choline chloride:water (1:1:6); and XoCH', xylitol:choline chloride:water (1:2:7.8), from López et al. (López et al., 2019). The standard deviations in the solubility measurements were: $\sigma(W_q)$=1.1·10^{-3} and 4.5·10^{-6} for GCH and GCiH, respectively.

Table 1 The diffusion coefficients, D, at 298 K of several species in the DESs and diluted mixtures (10%DES+90% D_2O) were obtained: aliphatic hydrogens of d-glucose (G), mobile hydrogen of d-glucose ($\mathrm{OH-G}$), aliphatic hydrogens of choline chloride or citric acid (HBA), mobile hydrogens of choline chloride or citric acid ($\mathrm{OH}-HBA$), and water (W). The value of the standard deviation in the calculation of each diffusion coefficient is included in parentheses.

DES	$10^{11}D_{\mathrm{G}}$ /m^2·s^{-1}	$10^{11}D_{\mathrm{OH-G}}$ /m^2·s^{-1}	$10^{11}D_{HBA}$ /m^2·s^{-1}	$10^{11}D_{\mathrm{OH}-HBA}$ /m^2·s^{-1}	$10^{11}D_{\mathrm{W}}$ /m^2·s^{-1}
GCH	n.d.[a]	0.157 (β) (5.6·10^{-4}) 0.168 (α) (8.3·10^{-4})	0.126 (2.8·10^{-3})	0.144 (5.4·10^{-3})	1.73 (1.4·10^{-2})
Diluted GCH	5.53 (2.6·10^{-4})	-	7.82 (1.0·10^{-3})	-	178.7[b] (1.0·10^{-3})
GCiH	0.551 (9.8·10^{-4})	-	0.421 (1.7·10^{-3})	-	2.71[b] (1.0·10^{-2})
Diluted GCiH	44.95 (3.0·10^{-4})	-	44.76 (5.0·10^{-4})	-	172.4[b] (2.5·10^{-3})

[a]non-determined; [b]mobile OH are included in the water signal

Table 2 Experimental and calculated properties of GCH[a] and GCiH[b] (this work) and CiCH[c] (López et al., 2020) at T=298.15 K and p = 0.1 MPa. The combined expanded uncertainties are also included.

Experimental properties	GCH	GCiH	CiCH	Calculated properties	GCH	GCiH	CiCH
ρ/ kg·m^{-3}	1213.66 ±0.05	1392.51 ±0.05	1245.98 ±0.05	α_p/ kK^{-1}	0.42 ±0.04	0.51 ±0.04	0.51 ±0.05
u/ m·s^{-1}	2158.6 ±0.5	1883.3 ±0.5	1885.93 ±0.5	κ_s/ TPa^{-1}	170.91 ±0.04	202.47 ±0.05	225.65 ±0.05
n_D	1.49884 ±2·10^{-5}	1.46706 ±2·10^{-5}	1.45460 ±2·10^{-5}	L_f/ Å	0.263 ±0.002	0.281 ±0.002	0.297 ±0.002
$C_{p,m}$/ J·mol^{-1}·K^{-1}	342 ±3	162 ±2	133 ±1	R_m/ cm^3·mol^{-1}	22.6675 ±0.0005	11.4726 ±0.0002	11.9610 ±0.0002
γ/ mN·m^{-1}	78.7 ±0.8	69.3 ±0.7	68.6 ±0.7	f_m/ cm^3·mol^{-1}	54.554 ±0.002	29.870 ±0.001	32.157 ±0.001
η/ mPa·s	1196 ±12	491 ±5	75 ±1	ΔS_S/ mN·m^{-1}·K^{-1}	0.321 ±0.002	0.177 ±0.001	0.099 ±0.001
σ/ mS·cm^{-1}	0.741 ±0.007	0.081 ±0.001	5.43 ±0.05	ΔH_S/ mN·m^{-1}	165.0 ±0.8	131.4 ±0.7	98.2 ±0.5
				$E_{a,\eta}$/ kJ·mol^{-1}	59.3 ±0.10	67.1 ±0.14	38.9 ±0.06
				$E_{a,\sigma}$/ kJ·mol^{-1}	50.21 ±0.10	41.37 ±0.02	32.12 ±0.01

[a]Glucose:choline chloride:water(1:3:3)

[b]Glucose:citric acid:water(1:1:6.5)

[c]Citric acid:choline chloride:water(1:1:6)